Relativistic Self-Consistent-Field Calculation of the Wave Functions, Eigenvalues, Isotope Shifts, and the 6s Hyperfine-Structure Coupling Constant as a Function of Pressure for Metallic Gold in the Wigner-Seitz Model

THOMAS C. TUCKER, LOUIS D. ROBERTS,* C. W. NESTOR, JR., AND THOMAS A. CARLSON
Oak Ridge National Laboratory,† Oak Ridge, Tennessee

AND

F. B. MALIK‡
Oak Ridge National Laboratory, Oak Ridge, Tennessee
and
Physics Department, Yale University, New Haven, Connecticut

(Received 3 June 1968)

We describe a versatile code for the calculation of the electronic properties of atoms in the Hartree-Dirac approximation. Calculations may be made for excited-state and multihole configurations as well as for the ground state of the neutral atom. Exchange may be included in the Slater approximation. The properties of metals may be calculated in the Wigner-Seitz approximation. The calculations may be made for a point nucleus or for a finite nucleus with a diffuse surface. We give results from a calculation made in the Wigner-Seitz approximation of the way a gold atom changes as a result of compression. This includes results about the way the charge density changes both near the gold nucleus and throughout the atom as the Wigner-Seitz radius is decreased from infinity to a value somewhat less than that for metallic gold at zero pressure. It was found that the charge density near the nucleus goes through a minimum which is related to the Wigner-Seitz boundary condition. The eigenvalues for all of the states occupied in atomic gold are given as a function of compression, of Slater exchange, and of nuclear size. Using these, the change with nuclear size of the eigenvalues of all of the electronic s states is calculated and is compared with a first-order perturbation-theory calculation of this change. The hfs coupling constant of the $6s$ state of a free atom of gold is calculated and compared with experiment. The core polarization in gold is discussed. Finally, a brief discussion of internal conversion in ^{169}Tm is given. The calculations given for gold are pertinent to a measurement of the change of energy of the resonance γ ray of ^{197}Au with pressure. This measurement was made through the use of the Mössbauer effect.

I. INTRODUCTION

In this paper we describe a code which treats the atomic many-body problem in the self-consistent field approximation using the Dirac equation to describe the motion of the individual electrons. The self-consistent potential is chosen to be of the Hartree type with the provision of incorporating the effect of the Pauli principle approximately in the form of an exchange potential. Within the framework of these approximations, this code can be used to compute the electronic structure of any atom in any given configuration, including two-hole states.[1] A number of relativistic self-consistent-field codes have recently become available.[2–8] Liberman *et al.*[2] have calculated the ground-state energies of a large number of elements. Tolliver *et al.*[3] and Hager *et al.*[8] have studied the internal-conversion problem using their code. Coulthard[7] did an extensive theoretical study of the eigenvalues of Hg in which he took the exclusion principle into account properly, i.e., in the sense of a complete integral kernel of the Fock type instead of as an exchange potential.

The code presented here includes as options the choice of a point or of a distributed nuclear charge, the choice of free-atom or of Wigner-Seitz[9] boundary conditions, and the choice of omitting the electron exchange interaction or of including it in the form of an approximate exchange potential.

We discuss an application of this code to the calculation of the wave functions of metallic gold as a function of compression. This application of the code was made to provide a basis for the interpretation of measurements of the γ-ray energy of gold as a function of pressure. This high-pressure work is described in another paper.[10]

---

* Present address: Physics Department, University of North Carolina, Chapel Hill, N. C.

† Operated by Union Carbide under contract with the U. S. Atomic Energy Commission.

‡ Work (Yale Report No. 2726-518) supported in part by the U. S. Air Force Office of Scientific Research and the U. S. Atomic Energy Commission under Contract No. AT(30-1)2726.

[1] C. W. Nestor, Jr., T. C. Tucker, T. A. Carlson, L. D. Roberts, F. B. Malik, and C. Froese, Oak Ridge National Laboratory Report No. ORNL-4027, 1966 (unpublished).

[2] D. Liberman, J. T. Waber, and D. T. Cromer, Phys. Rev. **137**, A27 (1965).

[3] C. L. Tolliver, C. P. Bhalla, and W. R. Garrett, Bull. Am. Phys. Soc. **11**, 512 (1966).

[4] J. L. Schonfelder, Proc. Phys. Soc. (London) **87**, 163 (1966).

[5] I. Lindgrin and A. Rosen, Institute of Physics of the Uppsala University Report No. UUIP-491, 1966 (unpublished).

[6] F. C. Smith and W. R. Johnson, Phys. Rev. **160**, 136 (1967).

[7] M. A. Coulthard, Proc. Phys. Soc. (London) **91**, 44 (1967).

[8] R. S. Hager and E. C. Seltzer, U. S. Atomic Energy Commission Report No. CALT-6360, 1967 (unpublished).

[9] E. P. Wigner and F. Seitz, Phys. Rev. **43**, 84 (1933); **46**, 509 (1934). A use of Wigner-Seitz boundary conditions for relativistic Hartree-Fock-Slater wave functions which differ somewhat from those in this paper has been investigated by J. T. Waber, D. Liberman, and D. T. Cromer, in *Proceedings of the Conference on Rare-Earth Research, Phoenix, Arizona*, edited by L. Eyring, (Gordon and Breach, Science Publishers, Inc., New York, 1965), p. 187.

[10] L. D. Roberts, D. O. Patterson, J. O. Thomson, and R. P. Levy, Phys. Rev. (to be published).

Our code is quite versatile and has a more general usefulness than is indicated by this specific application. For example, the code has been used to obtain wave functions to interpret Mössbauer measurements for Au [10] and for Ni and Ge,[11] to help in the interpretation of outer shell internal-conversion measurements[12] for ^{169}Tm, for an extensive calculation of electron shake-off probabilities[13] and for the calculation of certain properties of the superheavy elements.[14]

In Sec. II we give a detailed description of the theory related to the code, and in Sec. III we give results from calculations of the eigenenergies and wave functions of gold for both Wigner-Seitz and free-atom boundary conditions. This is done for atomic volumes ranging from infinity to somewhat less than the atomic volume of metallic gold. The way in which the wave functions of gold respond to compression is investigated and the relationship of these calculations to the high-pressure paper[10] is indicated. Brief discussions of the hfs coupling due to the 6s state in gold and internal-conversion coefficients for ^{169}Tm are given. In the Appendix we discuss a few interesting points related to the computation of wave functions and energy eigenvalues.

II. THEORY

A. Equations

In the relativistic self-consistent-field approximation the motion of each electron is described by a set of coupled radial wave equations of the Dirac type with a central electrostatic potential generated by the combination of the potential due to the nuclear charge, and the average potential originating from the mutual repulsion of electrons.[15,16] The motion of the ith electron in the field of other electrons and of the nucleus is given by

$$\frac{d}{dr}\begin{pmatrix}F_i(r)\\G_i(r)\end{pmatrix}=\begin{pmatrix}-k_i/r & \epsilon_i/\alpha-\alpha[V_N(r)-V_i(r)]\\(2-\epsilon_i)/\alpha+\alpha[V_N(r)-V_i(r)] & k_i/r\end{pmatrix}\begin{pmatrix}F_i(r)\\G_i(r)\end{pmatrix}, \tag{1}$$

where $F_i(r)=rf_i(r)$, $G_i(r)=rg_i(r)$, $f_i(r)$ and $g_i(r)$ are, respectively, the minor and major radial components of the wave function, and α is the fine-structure constant. We have used $\alpha=(137.0389)^{-1}$. k is the quantum number combining the total angular momentum j and the parity (determined by the angular momentum l), with

$$k=-(l-j)(2j+1). \tag{2}$$

The dimensionless energy eigenvalue ϵ_i associated with each electron in the ith orbit of energy E_i is given by

$$\epsilon_i=(mc^2-E_i)/mc^2, \tag{3}$$

where m and c are, respectively, the rest mass of the electron and the velocity of light. In Eq. (1), the radial distance r is expressed in Bohr units, $a_H=\hbar^2/me^2$. The potential functions $V_N(r)$ and $V_i(r)$ represent, respectively, the potential generated by a nucleus of total charge Z and the potential originating from the interaction of the electrons. In the Hartree approximation we use

$$V_i(r)=V_{Hi}(r), \tag{4}$$

with

$$V_{Hi}(r)=\frac{1}{r}\sum_{n'l'j'}q_{n'l'j'}Y_0(n'l'j';r)-\frac{1}{r}Y_0(nlj;r), \tag{5}$$

where $(nlj)\equiv i$ specifies the quantum numbers of the electron in the ith subshell, $q_{n'l'j'}$ is the number of electrons in the subshell specified by the quantum numbers $(n'l'j')$, and $Y_0(nlj;r)$ is given by

$$Y_0(nlj;r)=\int_0^r[F_{nlj}^2(r')+G_{nlj}^2(r')]dr'+r\int_r^\infty[F_{nlj}^2(r')+G_{nlj}^2(r')]\frac{dr'}{r'}. \tag{6}$$

For a point nucleus the nuclear potential function is Z/r, where Z is the atomic number, or total nuclear charge. However, where we are interested in the study of the effect of finite nuclear size on the electronic motion, the nuclear potential function can be expressed in terms of a nuclear charge distribution function ρ_N by

$$V_N(r)=\frac{1}{r}\int_0^r 4\pi r'^2\rho_N(r')dr'+\int_r^\infty 4\pi r'\rho_N(r')dr', \tag{7}$$

where ρ_N is normalized such that

$$4\pi\int_0^\infty r^2\rho_N(r)dr=Z, \tag{8}$$

with Z the total nuclear charge.

The Hartree potential, Eq. (5), neglects the effect of the exclusion principle which yields in addition to Eq. (5) a nonlocal potential. A simple approximate local form of this nonlocal potential has been obtained by Dirac[16,17] on the basis of the statistical theory of atomic

[11] G. Czjzek, J. L. C. Ford, Jr., J. C. Love, F. E. Obenshain, and H. H. F. Wegener, Phys. Rev. **174**, 331 (1968).
[12] T. A. Carlson, P. Erman, and K. Fransson, Nucl. Phys. (to be published).
[13] T. A. Carlson, C. W. Nestor, Jr., T. C. Tucker, and F. B. Malik, Phys. Rev. **169**, 27 (1968).
[14] T. C. Tucker, L. D. Roberts, C. W. Nestor, Jr., T. A. Carlson, and F. B. Malik, Phys. Rev. **174**, 118 (1968).
[15] B. Swirles, Proc. Roy. Soc. (London) **A152**, 625 (1935).
[16] P. A. M. Dirac, Proc. Cambridge Phil. Soc. **26**, 376 (1930).
[17] For a detailed discussion, see P. Gombas, in *Handbuch der Physik*, edited by S. Flügge (Springer-Verlag, Berlin, 1956), Vol. 36, p. 109.

structure. This exchange potential may be expressed in terms of the electronic charge density distribution $\rho_e(r)$ as

$$V_{ex}(r)=[3\rho_e(r)/\pi]^{1/3}. \quad (9)$$

When the exchange potential is incorporated, the total potential due to electron interaction is

$$V_i(r)=V_{Hi}(r)-V_{ex}(r)+r^{-1}Y_0(nlj,r). \quad (10)$$

The potential Eq. (10) tends to zero exponentially as the radial coordinate of the electron under consideration becomes large, whereas with N electrons the correct asymptotic form of the potential for the free atom is $(Z-N+1)/r$. Therefore, we have followed the prescription of Latter[18] to obtain the correct asymptotic form in free-atom calculations. No correction to Eq. (10) is needed for the Wigner-Seitz case. Since the form Eq. (9) for the exchange potential is an approximate one provision has been made in our code to use any multiple ζ of Eq. (9). For $\zeta=\frac{3}{2}$, the exchange potential is identical with the one proposed by Slater.[19]

B. Boundary Conditions

The electron radial wave functions for a free atom extend to all space, and hence are subject to the normalization condition

$$\int_0^\infty [F_i^*(r)F_i(r)+G_i^*(r)G_i(r)]dr=1. \quad (11)$$

Asymptotically these wave functions fall off at large r like a Dirac hydrogenic wave function with a central potential $(Z-N+1)/r$.

In a pure metal, because of the translational invariance of the lattice, the wave function of an electron of momentum $\mathbf{k}$ and position vector $\mathbf{r}$ will have the Bloch form $U_{\mathbf{k}}(\mathbf{r})e^{i\mathbf{k}\cdot\mathbf{r}}$. So far as we are aware, no calculation of $U_{\mathbf{k}}(\mathbf{r})$ has ever been made in which self-consistency was required for all of the shells of the atom. This complete self-consistency has been required for the calculations presented here. Some years ago, Wigner and Seitz[10] gave an approximate treatment of several metallic properties in which they used a model wave function $U_0(r)e^{i\mathbf{k}\cdot\mathbf{r}}$, where $U_0(r)\cong U_{\mathbf{k}}(\mathbf{r})(\mathbf{k}=0)$. The latter equality is only approximate in the Wigner-Seitz model because the polyhedral cell of volume V surrounding an atom on which the boundary conditions of $U_{\mathbf{k}}(\mathbf{r})$ are defined is replaced by a sphere of radius R_{WS}, where $\frac{4}{3}\pi R_{WS}^3=V$. In the calculations of Wigner and Seitz $U_0(r)$ was calculated in the Hartree-Schroedinger approximation under the boundary conditions that $(dU_0/dr)_{R_{WS}}=0$ and

$$\int_0^{R_{WS}} dr\, r^2U_0^2(r)=1.$$

This model has been widely used in the approximate theoretical treatment of many metallic properties.

At high atomic number relativistic effects become important, for example, in the calculation of the electron charge density near the nucleus or in the calculation of hyperfine structure coupling. To obtain an approximate calculation of these quantities for metallic systems we have obtained a solution to the Hartree-Dirac problem in a Wigner-Seitz type of approximation.

Since the major component g of the relativistic wave function corresponds to the nonrelativistic solution, we have chosen g to satisfy the boundary conditions

$$dg(r)/dr|_{r=R_{WS}}=0 \quad \text{for even } l \quad (12a)$$

and

$$g(r)|_{r=R_{WS}}=0 \quad \text{for odd } l \quad (12b)$$

with the normalization condition

$$\int_0^{R_{WS}} [F_i^*(r)F_i(r)+G_i^*(r)G_i(r)]dr=1. \quad (13)$$

In Eqs. (12) we have specified the boundary condition for the large component only. One might wish intuitively to specify a boundary condition on both components, for example, $f'=g'=0$ at R_{WS}. This is not possible, however. With two boundary conditions, the solutions to the Dirac equations, which are of first order, are overdetermined. Since most of the electron density in the outer region of the atom is contributed by the major component, it is believed that this choice of boundary conditions gives a useful approximation to the metallic wave functions at the bottom of the band.

The choice of boundary conditions [Eqs. (12)] is not unique. Another and possibly better choice in some cases would require Eq. (12a) to apply for all l, for example. Qualitatively, condition Eq. (12a) will approximate a bonding, and Eq. (12b), a nonbonding wave function. For gold our use of Eqs. (12) should be satisfactory since only states of even l have an appreciable amplitude at R_{WS}. For s-p metals such as Sn, on the other hand, the requirement (12a) for all l may give a better wave function and energy. We expect to include a choice of boundary conditions of this type in the next version of the program.

The nature of the solution of Eq. (1) for a point nucleus differs near the origin from that for a finite nucleus because of the different potential at the origin in these two cases.[20] For a point nucleus the nuclear potential has a $1/r$ singularity at $r=0$, but for a finite nucleus the potential tends to a constant at the origin. The potential caused by the distributed electron charge can be represented very close to the origin by

$$u=\lim_{r\to 0} V_i(r). \quad (14)$$

[18] R. Latter, Phys. Rev. **99**, 510 (1955).
[19] J. C. Slater, Phys. Rev. **81**, 385 (1951).
[20] F. G. Werner and J. A. Wheeler, Phys. Rev. **109**, 126 (1958).

Using this electron potential and a point nucleus, one can represent the wave functions near the origin by

$$\begin{pmatrix} F(r) \\ G(r) \end{pmatrix} = r^{\gamma} \begin{pmatrix} \sum_{n=0}^{\infty} a_n r^n \\ \sum_{n=0}^{\infty} b_n r^n \end{pmatrix}, \tag{15}$$

with

$$\gamma = (|k|^2 - \alpha^2 Z^2)^{1/2}, \tag{16}$$

$$b_0/a_0 = -(\gamma - k)/\alpha Z, \tag{17a}$$

and

$$\begin{pmatrix} a_n \\ b_n \end{pmatrix} = \frac{1}{n(n+2\gamma)} \begin{pmatrix} -\alpha Z & n+\gamma-k \\ n+\gamma+k & \alpha Z \end{pmatrix} \times \begin{pmatrix} [(2-\epsilon)/\alpha - \alpha u] a_{n-1} \\ (\epsilon/\alpha + \alpha u) b_{n-1} \end{pmatrix}. \tag{17b}$$

This is the standard solution, originally derived by Darwin[21] and by Gordon[22] for hydrogenic atoms.

Although the expansion Eq. (15) has been used widely in first-order perturbation calculations of the influence of finite nuclear size on various observables, e.g., the isomer shift in the Mössbauer effect,[23] the actual character of the solution near the origin is quite different from Eq. (15) for a finite nucleus.

In the discussion of the effect of a finite nucleus on the electron wave functions and eigenvalues, we have chosen to use a slight modification of the "smoothed uniform" charge distribution, used first for a nuclear charge distribution by Yennie, Ravenhall, and Wilson,[24] and subsequently by Elton,[25] and others. This distribution,

$$\rho_N(r) = C_N(1+e^{(r-r_0)/a})^{-1}, \tag{18}$$

has a small, but nonzero first derivative at the origin. Here r_0 is the radius at which the density is $\frac{1}{2}C_N$ (the "average" radius) and a gives a measure of the diffuseness of the nuclear surface. For a real nucleus one would expect the above derivative to be zero at the origin. To achieve this, we have used the distribution

$$\rho_N(r) = \eta_0 + \eta_2 r^2 \quad \text{for } 0 \le r \le r_m, \tag{19a}$$

$$\rho_N(r) = C_N(1+e^{(r-r_0)/a})^{-1} \quad \text{for } r_m \le r, \tag{19b}$$

where r_0 and a are those from the distribution Eq. (18), r_m is much less than r_0, and coefficients η_0, η_2, and C_N are chosen such that ρ_N is continuous with continuous first derivative at $r=r_m$ and the normalization equation [Eq. (8)] is satisfied. We have generally used $r_m \approx 0.1\, r_0$ in our calculations, although distributions Eqs. (18) and (19) differ only slightly for all $r_m < r_0 - 3a$.

[21] G. G. Darwin, Proc. Roy. Soc. (London) **A118**, 654 (1928).
[22] W. Gordon, Z. Physik **48**, 11 (1928).
[23] H. Frauenfelder, *The Mössbauer Effect* (W. A. Benjamin, Inc., New York, 1962).
[24] D. R. Yennie, D. G. Ravenhall, and R. N. Wilson, Phys. Rev. **95**, 500 (1954).
[25] L. R. B. Elton, *Nuclear Sizes* (Oxford University Press, Oxford, 1960).

For the density distribution Eq. (19), the nuclear potential at a distance less than r_m can be written as

$$V_N(r) = 4\pi\left(\frac{\eta_0 r_m^2}{2} + \frac{\eta_2 r_m^4}{4} - \frac{\eta_0 r^2}{6} - \frac{\eta_2 r^4}{20} + \int_{r_m}^{\infty} r'' \rho_N(r'') dr''\right), \tag{20a}$$

and setting

$$\nu_0 = 4\pi\left(\frac{\eta_0 r_m^2}{2} + \frac{\eta_2 r_m^4}{4} + \int_{r_m}^{\infty} r'' \rho_N(r'') dr''\right),$$

$$\nu_2 = -\tfrac{2}{3}\pi\eta_0,$$

$$\nu_4 = -\tfrac{1}{5}\eta_2,$$

we rewrite the potential as

$$V_N(r) = \nu_0 + \nu_2 r^2 + \nu_4 r^4 \quad (r \le r_m). \tag{20b}$$

Since the nuclear potential Eq. (20b) contains terms through r^4, little extra effort is required if the limiting electron potential (14) is replaced by the first terms of a Taylor's series about the origin for $V_i(r)$. It may be shown that using nuclear potential Eq. (20b) gives, through terms in r^4,

$$V_i(r) = \alpha_0 + \alpha_2 r^2 + \alpha_4 r^4 \quad \text{for } r \le r_m. \tag{21}$$

Then, defining $\sigma_i = \nu_i - \alpha_i$, the net potential sufficiently near the origin can be written

$$V_N(r) - V_i(r) = \sigma_0 + \sigma_2 r^2 + \sigma_4 r^4. \tag{22}$$

Using potential Eq. (22) we expand the wave functions near the origin by

$$\begin{pmatrix} F(r) \\ G(r) \end{pmatrix} = r^s \sum_{n=0}^{\infty} \begin{pmatrix} a_n \\ b_n \end{pmatrix} r^n. \tag{23}$$

Substituting expansion Eq. (23) into the Dirac equation [Eq. (1)] and equating the coefficients of equal powers of r gives the index s and the coefficients a_n and b_n:

$$s = |k|, \tag{24}$$

$$a_0 = p(s-k), \tag{25a}$$

$$b_0 = p(s+k), \tag{25b}$$

$$a_n = [(\epsilon/\alpha - \alpha\sigma_0) b_{n-1} - \alpha\sigma_2 b_{n-3} - \alpha\sigma_4 b_{n-5}]/(s+k+n), \tag{25c}$$

$$b_n = [((2-\epsilon)/\alpha + \alpha\sigma_0) a_{n-1} + \alpha\sigma_2 a_{n-3} + \alpha\sigma_4 a_{n-5}]/(s-k+n), \tag{25d}$$

where p is a normalizing factor, and subject to the condition

$$a_{n-i} = b_{n-i} = 0 \quad \text{for } n < i,\ i = 1,\ 3, \text{ or } 5.$$

From Eqs. (23)–(25) it is seen that one wave function component contains only odd powers of r while the other has only even powers. The self-consistency of the electron potential Eq. (20) is evident if wave functions Eq. (23) are used in Eqs. (6) and (9).

An important difference in the behavior of the wave functions for a point and a finite nucleus is that for a point nucleus the first power of r in the Darwin expansion Eq. (15) is $(k^2-\alpha^2Z^2)^{1/2}$, which is nonintegral, and both leading coefficients are nonzero. For a finite nucleus with ρ_N given by Eqs. (19), however, the first power of r in expansion Eq. (23) is an integer $|k|$ and depending upon the sign of k, either a_0 or b_0 is zero. Although we have used a very specific nuclear charge distribution [Eq. (19)] to obtain the wave functions Eq. (23) near the origin, it is important to notice that the qualitative differences in leading coefficients and powers of r for point and finite nuclei are independent of the particular charge density used for the finite nucleus. These differences occur because the $1/r$ singularity of the point nucleus potential is replaced by a finite value in a finite nucleus. The qualitative difference between Eqs. (15) and (23) will manifest itself in the computation of the effect of finite nuclear size on any measurable quantity involving the electronic charge distribution in the interior of a nucleus. Expansion Eq. (23) has been used in the finite-nuclear-size calculations given in Sec. III.

III. INTERPRETATION OF HIGH-PRESSURE MÖSSBAUER-EFFECT MEASUREMENTS FOR METALLIC GOLD THROUGH CALCULATION OF ELECTRON CHARGE DENSITIES, EIGENVALUES, AND 6*s* HFS COUPLING

A. Introduction

In this section we present some results from a series of calculations of the electron eigenvalues and charge densities of atomic gold and of the way that these change when a gold sample is compressed from infinite atomic volume to an atomic volume somewhat less than that of metallic gold. These calculations were made to provide a basis for the interpretation of a measurement[10] —made through the use of the Mössbauer effect[23]—of the pressure dependence of the energy E_γ of the resonance γ ray of metallic gold. The results from the extensive printout of information given by the code which we shall present here are those which have a particular bearing on this Mössbauer-effect measurement and also on the way the gold-atom charge-density distribution responds to the compression of the atom.

The electrons and nucleons within an atom constitute a single interacting system, and the energy of a state t of this system $E_t(\zeta,\xi)$ depends at once on all of the electron and nucleon coordinates ξ and ζ. All of the quantum numbers of the system are included in t. The energy of a γ ray depends then not only on the nuclear coordinates but on the coordinates of the electrons as well. Because of this, a sufficiently precise measurement of E_γ can be interpreted to give information about the electron charge density near the nucleus. The Mössbauer method[23] provides a tool for making such precise measurements of E_γ.

In a first-order perturbation-theory treatment it may be assumed that the energy $E_t(\zeta,\xi)$ may be written in the form

$$E_t(\zeta,\xi)=E_n(\zeta)+E_e(\xi)+e(\zeta,\xi). \tag{26}$$

In this approximation the energy $E_n(\zeta)$ associated with the nuclear coordinates is taken to be independent of the electron coordinates. The energy $E_e(\xi)$ of the electron states is calculated for an assumed point nucleus, and is thus forced to be independent of the nuclear coordinates. The nucleus is, of course, finite in radius, and the Coulomb interaction between the actual finite nucleus and the atomic electrons is weaker than for the point-nuclear case assumed in the above calculation of $E_e(\xi)$. Thus a term $e(\zeta,\xi)$ must be included in Eq. (26) if the calculated energy $E_t(\zeta,\xi)$ is to be compared with precise measurements.

In the following we shall calculate the energies $E_e(\xi)$ and $e(\zeta,\xi)$, and the electron radial probability density

$$|\psi_{R\mathrm{WS}}(r)|^2=|f_{R\mathrm{WS}}(r)|^2+|g_{R\mathrm{WS}}(r)|^2$$

for gold metal in the Hartree-Dirac-Wigner-Seitz or in the Hartree-Dirac-Slater-Wigner-Seitz model. A subscript R_{WS}, e.g., in $|\psi_{R\mathrm{WS}}(r)|^2$, designates the Wigner-Seitz radius for which the calculation was made.

When a pressure p is applied to the gold sample the atomic volume $V=\frac{4}{3}\pi R_{\mathrm{WS}}^3$ is reduced, and this reduction may be described in terms of the compressibility

$$K(p)=-\frac{1}{V}\frac{dV}{dp}=-\frac{3}{R_{\mathrm{WS}}}\frac{dR_{\mathrm{WS}}}{dp}.$$

The dominant behavior of the energy e may be described in terms of the nuclear radius r_0 and the electron probability density at the nuclear surface $|\psi_{R\mathrm{WS}}(r_0)|^2$ as parameters. Thus we shall write $e=e(r_0,|\psi_{R\mathrm{WS}}(r_0)|^2)$. When the radius of the excited state of a nucleus r_{0e} is different from that of the ground state r_{0g}, the resonant γ-ray energy E_γ will depend on this difference. Thus the resonant γ-ray energy for a Wigner-Seitz radius R_{WS} is

$$E_{\gamma R\mathrm{WS}}=E_{ne}(\zeta)-E_{ng}(\zeta)+e(r_{0e},|\psi_{R\mathrm{WS}}(r_{0e})|^2)-e(r_{0g},|\psi_{R\mathrm{WS}}(r_{0g})|^2), \tag{27}$$

where the $E_{ng}(\zeta)$ and $E_{ne}(\zeta)$ refer to the ground and first excited states of the nucleus. In our high-pressure Mössbauer studies[10] we have measured the difference

$$\begin{aligned}\Delta E&=E_{\gamma R\mathrm{WS}}-E_{\gamma R_0\mathrm{WS}}\\&=[e(r_{0e},|\psi_{R\mathrm{WS}}(r_{0e})|^2)-e(r_{0g},|\psi_{R\mathrm{WS}}(r_{0g})|^2)]\\&\quad-[e(r_{0e},|\psi_{R_0\mathrm{WS}}(r_{0e})|^2)-e(r_{0g},|\psi_{R_0\mathrm{WS}}(r_{0g})|^2)],\end{aligned} \tag{28}$$

where $R_{0\mathrm{WS}}$ and R_{WS} are the Wigner-Seitz radii for gold at zero applied pressure and when the sample has been compressed. In Mössbauer-effect studies, ΔE is often referred to as the isomer shift.[23]

Our specific purpose, then, is to calculate e. We shall

do this in two ways: (a) as an explicit function of r_0 and of $|\psi_{R_{WS}}(r_0)|^2$ by a method described by Breit,[26] and (b) through direct calculations of the eigenvalues of the Dirac equations for a gold atom first with a finite nucleus of radius r_0 and second with a point nucleus, both with the same R_{WS}. For the first method, a calculation of $|\psi_{R_{WS}}(r)|^2$ for an atom which is assumed to have a point nucleus is used.

Near the nucleus only $s_{1/2}$ and $p_{1/2}$ states contribute appreciably to $|\psi_{R_{WS}}(r)|^2$. For a calculation in which a point nucleus is assumed, this charge density near the nucleus may be obtained from Eq. (15), and in general takes the form

$$|\psi_{R_{WS}}(r)|_{nj}^2=r^{2\gamma-2}\sum_{\alpha=0}^{\infty}C_{nj\alpha}(R_{WS})r^{\alpha}. \quad (29)$$

The $C_{nj\alpha}(R_{WS})$ are a set of numbers with a summation index α which characterize the charge density as a function of R_{WS}, for a state of principal quantum number n and angular momentum j. In addition to giving a numerical solution to the Dirac equations for $0\leq r\leq R_{WS}$, the code gives a calculation of the first 12 terms in this series. From the calculation of the $C_{nj\alpha}$ it may be seen that, for the range $0\leq r\leq\sim r_0$, the first term $C_{nj0}(R_{WS})r^{2\gamma-2}$ gives the charge density surrounding a point nucleus to within a few percent. We will use the abbreviation $C_{nj}(R_{WS})=C_{nj0}(R_{WS})$, and much of the following discussion will be relative to this quantity. As we shall see, only $C_{6s}(R_{WS})$ will change appreciably with R_{WS} for $R_{WS}\sim R_{0WS}$.

As we mentioned above, Breit[26] has given a first-order perturbation-theory calculation of e. In this calculation, he assumed a spherical nucleus of uniform density with radius r_0 and an electron charge density given by $|\psi(r)|_{nj}^2=C_{nj}(R_{WS})r^{2\gamma-2}$ (atomic units) for a point nucleus. In terms of our notation his result may be written

$$e_{nj}{}^{B}(r_0,R_{WS})=\frac{3C_{nj}(R_{WS})}{\gamma(2\gamma+1)(2\gamma+3)}\left(\frac{Ze^2}{2a_H}\right)\left(\frac{r_0{}^{\gamma}}{a_H}\right)^{2\gamma} \quad (30)$$

and the isomer shift ΔE; Eq. (28) may be given in a form suitable for use in the discussion of our high-pressure studies[10]:

$$\Delta E_{nj}=\frac{6}{(2\gamma+1)(2\gamma+3)}\left(\frac{Ze^2}{2a_H}\right)(C_{nj}(R_{0WS})r_0{}^{2\gamma})\times\left(\frac{d\ln C_{nj}}{d\ln R_{WS}{}^{-3}}\right)_{R_{0WS}}\left(\frac{\Delta r_0}{r_0}\right)\left(\frac{\Delta R_{WS}{}^{-3}}{R_{WS}{}^{-3}}\right). \quad (31)$$

In the interpretation of our high-pressure measurements through the use of Eqs. (30) and (31) we shall then need to calculate $C_{nj}(R_{WS})$ and

$$(d\ln C_{nj}/d\ln R_{WS}{}^{-3})_{R_{0WS}}.$$

[26] G. Breit, Rev. Mod. Phys. **30**, 507 (1958).

The numerical calculation of $|\psi_{R_{WS}}(r)|^2$ for the whole range of r, $0\leq r\leq R_{WS}$ will also be of interest in gaining an understanding of the behavior of the function $C_{nj}=C_{nj}(R_{WS})$. The application of these calculated results to the interpretation of our high-pressure measurements is given in another paper.[10] The Wigner-Seitz model gives a good approximation to the metallic wave function only at the bottom of the band. Thus the results given here should be regarded as an interim treatment. It will be most useful to obtain a full band-theory calculation of the problem.

B. Calculations of $|\psi_{R_{WS}}(r)|^2$ and $C_{ns}(R_{WS})$ for a Point Nucleus as a Function of the R_{WS}

Calculations of $|\psi_{R_{WS}}(r)|^2$ and of $C_{ns}(R_{WS})$ have been made for values of R_{WS} in the range $2.9\leq R_{WS}\leq\infty$, where R_{WS} is in Bohr units. The Wigner-Seitz radius for metallic gold at zero pressure is $R_{0WS}=3.00$ Bohr units. All of the values for C_{nj} were calculated for a point nucleus for use in the calculation of $e(r_0,R_{WS})$ in the Breit approximation.

Most of the calculations were made with the Hartree potential [Eqs. (4) and (5)], although a few calculations were made with the exchange approximation of Eqs. (9) and (10). This was because an early version of the code with which most of the $C_{nj}(R_{WS})$ calculations were made did not include the exchange potential $V_{ex}(r)$. This omission of V_{ex} does not give a serious error in the calculation of $e(r_0,R_{WS})$, however, for $C_{ns}(R_{WS})$ has only a weak dependence on V_{ex}. For example, with a point nucleus and with $R_{WS}=3.010239$ atomic units $C_{6s}=66.67$ with $V_{ex}(r)=0$, and $C_{6s}=67.24$ with $V_{ex}(r)$ as given in Eq. (9) included in the calculation.

In Table I we give values for $C_{nj}(R_{WS})$ for all of the $s_{1/2}$ and $p_{1/2}$ states occupied in atomic gold for R_{WS} values of ∞, 3.000000, and 2.899999. Between $R_{WS}=3.000000$ and $R_{WS}=2.899999$, which is a large compression compared to present experimental capabilities, it is found that the total charge density near the nucleus due to all of the inner shells is constant to within the precision of the calculation of a few parts in 10^6. Only

TABLE I. This table gives $C_{nj}(R_{WS})$ near a point nucleus $|\psi_{R_{WS}}(r)|^2\cong C_{nj}(R_{WS})r^{2\gamma-2}$ for all of the $s_{1/2}$ and $p_{1/2}$ states for atomic gold for the free atom and for two values of R_{WS} near metallic gold. R_{WS} is the Wigner-Seitz radius.

Electron quantum state	$C_{nj}(\infty)$	$C_{nj}(3.000000)$	$C_{nj}(2.899999)$
$1s_{1/2}$	414 529.55	414 527.53	414 527.62
$2s_{1/2}$	61 624.07	61 623.86	61 623.88
$2p_{1/2}$	4 356.15	4 356.09	4 356.05
$3s_{1/2}$	13 973.45	13 974.01	13 974.07
$3p_{1/2}$	1 100.78	1 100.84	1 100.84
$4s_{1/2}$	3 552.47	3 553.26	3 553.31
$4p_{1/2}$	274.51	274.59	274.59
$5s_{1/2}$	700.25	705.35	705.32
$5p_{1/2}$	47.21	48.00	48.08
sum	500 158.44	500 163.77	500 163.53
$6s_{1/2}$	40.14	67.27	73.68

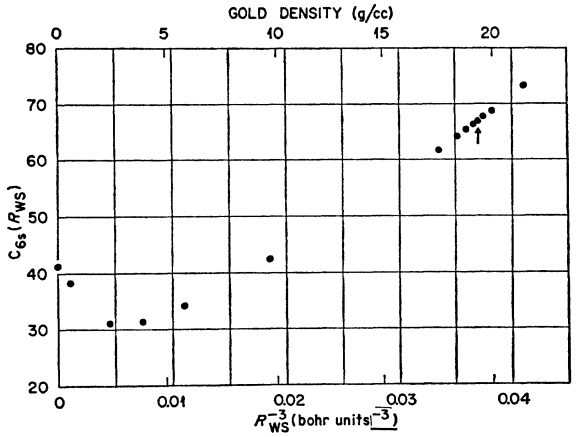

FIG. 1. The electron charge density near a point nucleus may be represented in good approximation by $|\psi(r)|^2 = Cr^{2\gamma-2}$. Here $C_{6s}(R_{WS})$ for gold is plotted versus $1/R_{WS}^3$ and also versus the gold average density in g/cc. R_{WS} is the Wigner-Seitz radius. This graph gives C_{6s} for atomic gold, for gold metal, and for the whole range of $1/R_{WS}^3$ in between. It shows that in the intermediate range of $1/R_{WS}^3$, C may be expected to go through a minimum. The arrow corresponds to R_{WS} for metallic gold.

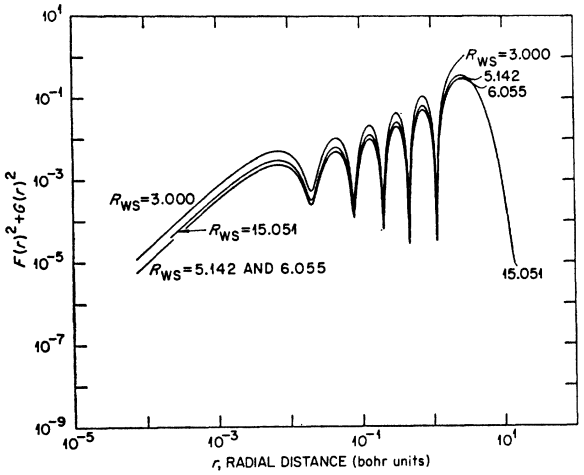

FIG. 3. Radial probability density function for the gold $6s_{1/2}$ state as a function of radius r and of Wigner-Seitz radius R_{WS}. This graph illustrates in a more complete way the result which is shown in Fig. 1, namely, that, as the atom is compressed, the 6s charge at first may be expected to move outward and then inward again with decreasing R_{WS}.

$C_{6s}(R_{WS})$ is found to change appreciably with R_{WS}. This is a very helpful result, for it implies that

$$(d\ln C_{nj}/d\ln R_{WS}^{-3})_{R_{0WS}} \sim 0$$

for all of the inner shells and that our high-pressure γ-ray-energy measurements[10] can be interpreted in terms of $C_{6s}(R_{WS})$ alone without direct reference to the inner shell electrons.

Figure 1 is a graph of $C_{6s}(R_{WS})$, which is proportional to the electron charge density near the nucleus, versus the average "metallic" density. Most of this graph is for low metallic or Wigner-Seitz density values but this low-density range is of interest in gaining an understanding in detail of how the atom, in the Wigner-Seitz model, responds to compression.

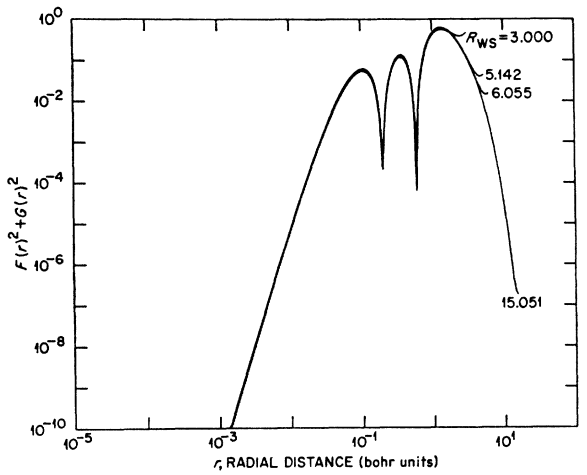

FIG. 2. Radial probability density function for the gold $5d_{5/2}$ state as a function of radius r and of the Wigner-Seitz radius R_{WS}. As R_{WS} is decreased, i.e., as the atom is compressed, the $5d_{5/2}$ charge which is displaced inward tends to pile up near the inner surface of the Wigner-Seitz sphere. In the inner region of the atom the $5d_{5/2}$ charge changes only slightly with compression. The $5d_{3/2}$ charge density behaves in a similar way.

As R_{WS} is decreased from infinity, the average metallic density correspondingly is increased from zero, and in the Wigner-Seitz model the electron probability density near the nucleus at first decreases to a minimum near an average metallic gold density of 3 g/cm^3 and then increases monotonically.

For the interpretation of the high-pressure measurements, we need the value for the logarithmic derivative in Eq. (31). This derivative is related to the rate of change of the electron charge density near the gold nucleus with respect to the average metallic density. We find that

$$(d\ln C_{6s}/d\ln R^{-3})_{R_{0WS}} = 0.86, \qquad (32)$$

where the subscript means that the derivative has been evaluated at the density of metallic gold of 19.3 g/cm^3 or more precisely for the range $2.97 \leq R_{WS} \leq 3.00$ Bohr units.

The dip in the curve of C versus R_{WS}^{-3} is noteworthy because one might at first expect that the charge density

TABLE II. The charge density near the proton in hydrogen calculated with Wigner-Seitz boundary conditions. Near the proton $|\psi_{RWS}(r)|^2 \cong C_{1s}(R_{WS})r^{2\gamma-2}$. $C_{1s}(R_{WS})$ is given versus V^{-1} with $V = \frac{4}{3}\pi R_{WS}^3$. R_{WS} is the Wigner-Seitz radius.

V	$1/V$	C_{1s}
∞	0	4.0000475
125.02280	0.007999	3.9873027
19.17287	0.0521570	3.0495676
5.16031	0.1937868	2.5564446
2.94025	0.3401071	2.8175614
2.02081	0.494851	3.1673774
0.95456	1.047603	4.4273013

near the nucleus would increase monotonically with the average gold density. This effect arises mostly from the nature of the Wigner-Seitz boundary condition but also in part from the change of $5d$ electron screening with R_{WS}. This is discussed further below.

In Fig. 2 we give a plot of the $5d_{5/2}$ radial probability density function versus r on a log-log plot for four values of R_{WS}, namely, 3.000, 5.142, 6.055, and 15.051 Bohr units. This graph illustrates the fact that for the $5d_{5/2}$ state, as the radius of the Wigner-Seitz sphere is decreased, the charge which is displaced inward tends to pile up just inside the surface of this sphere, and also that the $5d_{5/2}$ charge density further within the atom is very little modified. This pile-up near the surface of the sphere is presumably related to the centrifugal force arising from the orbital motion of the electron.

In Fig. 3 we show the $6s_{1/2}$ radial probability density function as a function of r on the same type of log-log plot and for the same set of four Wigner-Seitz radii as in Fig. 2. Here the behavior, which is quite different from that of the d electron, is also qualitatively different for two different regions of r. For r values inside of r_η, the radius of the outermost node near one Bohr unit, the electron charge density in good approximation changes simply by a factor independent of r, i.e., in the sense of a normalization, as R_{WS} is changed. For r values greater than r_η, the radial dependence of the charge density changes with R_{WS}. As may be seen from Fig. 3, the charge density in the inner region of r has decreased, and for $r>r_\eta$ has moved outward for $R_{WS}=5.142$ and $R_{WS}=6.055$ relative to the charge density distributions for $R_{WS}=3.000$ and $R_{WS}=15.051$. This shows how the minimum in $C_{6s}(R_{WS})$ is related to an outward and then inward motion of the $6s$ charge as R_{WS} is decreased.

It is of interest to note that, as is to be expected, the nodes of the wave functions do not move appreciably as the atom is compressed.

In a strongly coupled many-electron system such as gold, it is difficult to separate the effects of screening and boundary conditions. To aid in this we have calculated $C_{1s}(R_{WS})$ for Wigner-Seitz hydrogen, for which there are of course no many-electron screening effects. The results of this calculation are shown in Table II. It is seen that here also $C_{1s}(R_{WS})$ first of all decreases but then increases again as the average density of Wigner-Seitz hydrogen is increased.

Returning to Fig. 2, we see again that with decreasing R_{WS} the $5d_{5/2}$ electrons tend to build up in the outer region of the atom. Qualitatively, this $5d$ screening charge build up for $r\sim R_{WS}$ will tend to force the $6s_{1/2}$ charge inward as R_{WS} decreases.

The Wigner-Seitz boundary condition which we have used requires that the slope of the large component of ψ_{6s} be zero at $r=R_{WS}$. As compared to the wave function of the free atom, the requirement that $(df/dr)_{R_{WS}}=0$ tends to "lift" or increase the amplitude $f(r)$ near $r=R$ and move charge outward in the normalized wave function when R_{WS} is large. For values of R_{WS} less than about 5 Bohr units, however, the effects of compression do become dominant, and the $6s$ charge density throughout the atom increases as R_{WS} decreases in this region. These facts imply that the minimum in $C(R_{WS})$ in Fig. 1 and in Table II is a characteristic of the Wigner-Seitz boundary condition.

C. Eigenvalues for Au as Function of R_{WS} and r_0

In Table III we show how the calculated eigenvalues for gold change when the atom is compressed, when the exchange potential [Eq. (9)] is introduced (with an exchange parameter $\zeta=1$), and when a finite nucleus is introduced. The measured binding energies[27] are also listed. The calculation for $R_{WS}=3.010239$ and including $V_{ex}(r)$ [Eq. (9)] and a finite nucleus gives our best approximation to metallic gold. A comparison between this calculation of the eigenvalues with the measured values shows an agreement within a few tenths percent for the $1s$ and $4f$ states. Otherwise the agreement is within 1–2% for L and M shells, within about 4% for the N shell and 4–6% for the 0 shell.

When we use the exchange parameter $\zeta=\frac{3}{2}$ with Eq. (9) and free-atom boundary conditions, our eigenvalues agree with those obtained by Liberman, Waber, and Cromer[2] in their comparable calculation to within a few hundredths percent.

The dependence of the eigenvalue of an atomic state on the nuclear size may be calculated with the code using Eqs. (19) to describe the nucleus. This nuclear size effect is illustrated in Table III, where calculated eigenenergies are shown for two Wigner-Seitz atoms which have $R_{WS}=3.010239$ and include $V_{ex}(r)$, but where $r_0=a=0$ in one case and $r_0=6.38$ F, $a=0.567$ F in the other. Here

$$e_{ns}(r_0,R_{WS})=E_{ns}(r_0\neq 0)-E_{ns}(r_0=0). \quad (33)$$

Table IV lists the $e_{ns}(r_0,R_{WS})$ obtained from Table III for these two cases through the use of Eq. (33).

Breit's formula [Eq. (30)] may be written in the form

$$\left(\frac{e_{ns}}{C_{ns}}\right)_B=\frac{3}{\gamma(2\gamma+1)(2\gamma+3)}\left(\frac{Ze^2}{2a_H}\right)\left(\frac{r_0}{a_H}\right)^{2\gamma}. \quad (34)$$

Thus, in this treatment, e_{ns}/C_{ns} depends only on the nuclear radius and on physical constants. For $r_0=6.38$ F and for gold with $Z=79$,

$$(e_{ns}/C_{ns})_B=1.274\times 10^{-4}, \quad (35)$$

where e_{ns} is in eV, and C is in atomic units. In Table IV we also list our calculated values for C_{ns}, the values of e_{ns} calculated from Table III and Eq. (33), and the ratio e_{ns}/C_{ns}. This ratio is seen to be nearly constant and about 20% smaller than the above value [Eq. (32)] obtained from perturbation theory. The small fluctu-

[27] J. A. Bearden and A. F. Burr, Rev. Mod. Phys. 39, 125 (1967).

TABLE III. Energy eigenvalues for gold calculated for various values of the nuclear radius r_0 and diffusivity a, the Wigner-Seitz radius R_{WS}, and with and without the exchange potential V_{ex} [Eq. (9)]. The experimental values corresponding to these eigenvalues are shown in the last column. The energies are in eV. 1 Ry = 13.6053 eV.

Shell	$R=\infty$ $r_0=0$ without V_{ex}	$R=3.010239$ $r_0=0$ without V_{ex}	$R=3.010239$ $r_0=0$ with V_{ex}, $\zeta=1$	$R=3.010239$ $r_0=6.38$ F $a=0.567$ F with V_{ex}, $\zeta=1$	Experimental binding energies
$1s_{1/2}$	8.121516×10^4	8.121674×10^4	8.059108×10^4	8.054601×10^4	80 724.9±0.5
$2s_{1/2}$	1.423277×10^4	1.423451×10^4	1.421182×10^4	1.420516×10^4	14 839.3±1.0
$2p_{1/2}$	1.369883×10^4	1.370056×10^4	1.363082×10^4	1.363065×10^4	13 733.6±0.3
$2p_{3/2}$	1.185487×10^4	1.185661×10^4	1.179708×10^4	1.179734×10^4	11 918.7±0.3
$3s_{1/2}$	3.347571×10^3	3.349057×10^3	3.355955×10^3	3.354444×10^3	3 424.9±0.3
$3p_{1/2}$	3.086957×10^3	3.088460×10^3	3.094513×10^3	3.094472×10^3	3 147.8±0.4
$3p_{3/2}$	2.685716×10^3	2.687196×10^3	2.689931×10^3	2.690002×10^3	2 743.0±0.3
$3d_{3/2}$	2.265301×10^3	2.266818×10^3	2.254980×10^3	2.255044×10^3	2 291.1±0.3
$3d_{5/2}$	2.178552×10^3	2.180090×10^3	2.167987×10^3	2.168048×10^3	2 205.7±0.3
$4s_{1/2}$	7.225551×10^2	7.238646×10^2	7.300208×10^2	7.296371×10^2	758.8±0.4
$4p_{1/2}$	6.109975×10^2	6.123054×10^2	6.186096×10^2	6.186002×10^2	643.7±0.5
$4p_{3/2}$	5.144000×10^2	5.156816×10^2	5.213144×10^2	5.213328×10^2	545.4±0.5
$4d_{3/2}$	3.340860×10^2	3.353725×10^2	3.388407×10^2	3.388554×10^2	352.0±0.4
$4d_{5/2}$	3.161874×10^2	3.174601×10^2	3.207105×10^2	3.207242×10^2	333.9±0.4
$5s_{1/2}$	1.109359×10^2	1.116857×10^2	1.108358×10^2	1.107582×10^2	107.8±0.7
$4f_{5/2}$	8.721970×10^1	8.846768×10^1	8.637980×10^1	8.638795×10^1	86.4±0.4
$4f_{7/2}$	8.338152×10^1	8.462104×10^1	8.255475×10^1	8.256357×10^1	82.8±0.5
$5p_{1/2}$	7.440365×10^1	7.496369×10^1	7.429439×10^1	7.429269×10^1	71.7±0.7
$5p_{3/2}$	5.751726×10^1	5.779117×10^1	5.721664×10^1	5.721960×10^1	53.7±0.7
$6s_{1/2}$	6.909459×10^0	1.159874×10^1	1.180646×10^1	1.179905×10^1	
$5d_{3/2}$	8.989940×10^0	1.024083×10^1	1.081404×10^1	1.081482×10	
$5d_{5/2}$	7.241904×10^0	8.885858×10^0	9.457758×10^0	9.458603×10	

[a] Reference 27.

ation of our calculated values for the ratio in Table IV may be in part because the energy difference [Eq. (33)] is near the limit of precision of our calculation of the eigenvalues which, like C_{ns}, is of the order of a few parts in 10^6.

An exact agreement between our value for e_{ns}/C_{ns} (Table IV) and the perturbation-theory result [Eq. (35)] is not expected. In addition to our calculations being more comprehensive and exact, the assumptions as to the nuclear shape and electron wave functions in the two calculations differ somewhat (see above and Sec. II). The comparison of the two results, however, provides some indication of the reliability of the perturbation-theory estimate for e_{ns} in the case of gold. For heavier elements this agreement will be increasingly poor.[14]

TABLE IV. The energy difference $e_{ns}(r_0,R_{WS})$ [Eq. (33)] between the atomic eigenvalues calculated for a finite and for a point nucleus for all of the $s_{1/2}$ states of gold. The calculations were made using our Dirac-Hartree-Slater-Wigner-Seitz code with an exchange parameter $\zeta=1$. C_{ns} gives a measure of the charge density near the nucleus; see Eq. (29). In first order $e_{ns}(r_0,R_{WS})/C_{ns}$ is expected to be a constant independent of the principal quantum number n. The energies are in eV. 1 Ry = 13.6053 eV.

State	$e_{ns}(r_0,R_{WS})$	C_{ns}	$10^4\times e_{ns}(r_0,R_{WS})/C_{ns}$
$1s$	45.07	413 961.16	1.088
$2s$	6.66	62 163.836	1.072
$3s$	1.510	14 229.379	1.061
$4s$	0.3837	3 630.7706	1.056
$5s$	0.0776	737.38189	1.052
$6s$	0.00741	67.242266	1.101
		average	1.073

The isomer shift [Eq. (28)] may be written in the convenient form

$$\Delta E_{ns}=\frac{\partial^2 E_{ns}(R,r_0,a)}{\partial R\partial r_0}\Delta R\Delta r_0. \tag{36}$$

The precision of our calculation of the eigenvalue E_{6s} of a few parts in 10^6 is not quite sufficient to obtain an adequate value for the second derivative $\partial^2 E_{ns}/\partial R\partial r_0$. Thus we have used the Breit treatment along with our value for $C_{6s}(R)$ and the value for the logarithmic derivative Eq. (32) in the interpretation of our high-pressure measurements.[10] It will be of much value in the future to perform atomic calculations with a somewhat higher precision so that it will be possible to obtain values for second derivatives of this type. In such calculations it will be desirable to include correlation and a more exact treatment of exchange.

D. Calculation of hfs Coupling for 6s State of Free Au Atom

In general in the discussion of Mössbauer isomer shift measurements, and also of measurements in numerous other areas in solid-state and nuclear physics, a value for $|\psi(r_0)|^2$ is very useful. Often a value for this quantity is obtained from the hfs coupling constant A [Eq. (37)] measured for the free atom. Here we have obtained a value for the $C_{nj}(R_{WS})$ and thus of $|\psi_{R_{WS}}(r_0)|^2$ for dgol in the Hartree-Dirac-Slater-Wigner-Seitz approximation, for all values of R_{WS} from ∞, the free atom, to $R_{WS}\sim R_{0WS}$ for metallic gold. Because of the intimate

relationship between C_{nj} and the hfs coupling constant, we give in this section a calculation of the hfs coupling for the free atomic $6s_{1/2}$ state of gold and compare this with the measured value. This comparison will serve to emphasize the fact that if $|\psi(r_0)|^2$ is estimated from A in the usual way,[28] a considerable error may occur unless the contributions of nuclear structure and atomic core electrons to the hfs coupling are taken into account. Also, an estimate of $|\psi(r_0)|^2$ from A will not usually take into account the change of this charge density as one goes from the free atom for which A is measured to the solid for which the charge density is frequently used. (See Fig. 1.)

For a point nucleus the hfs interaction may be written in the form[29]

$$\mathcal{H}_{\rm hfs}=A\mathbf{S}\cdot\mathbf{I}$$
$$=-\frac{4}{3}\frac{e\mu_n}{SIa_H^2}\int_0^\infty f(r)g(r)dr\,\mathbf{S}\cdot\mathbf{I}. \qquad (37)$$

Here e is the electron charge, μ_n is the nuclear magnetic moment, $\mathbf{S}$ and $\mathbf{I}$ are the electron and nuclear spin operators, and $S=\frac{1}{2}$ and $I=\frac{3}{2}$ are the eigenvalues for these appropriate to the ground state of gold. The integral is in atomic units. Using the functions $f(r)$ and $g(r)$ which we have obtained for the $6s_{1/2}$ state, we have calculated the value of the integral as

$$\int_0^\infty fgdr=-0.6137 \qquad (38)$$

atomic units. If we substitute this value for the integral in Eq. (37) along with the values for the required physical constants, we obtain a value for A of 2067 Mc/sec. The experimental value for A obtained from atomic beam measurements[30] is 3054 Mc/sec. Thus our value for A due to the $6s_{1/2}$ electron is some 30% lower than the experimental value. This does not mean, however, that our $6s_{1/2}$ wave function is correspondingly in error, because the contribution of the core electrons and the effects of nuclear size and structure have not yet been introduced into our hfs calculation.

In the case of the ^2S ground state of lithium, calculations of the hfs coupling in a restricted Hartree-Fock approximation give a calculated hfs interval of 579.1 and 627.0 Mc/sec,[31,32] compared to the experimental value of 803.512 Mc/sec.[33] When the contribution of the core electrons to the hfs coupling is taken into account through an unrestricted Hartree-Fock calculation, an interval of 781.1 Mc/sec is obtained,[32] and the use of the Bethe-Goldstone equation leads to a calculated interval of 801.1 Mc/sec.[34]

Our calculation is a restricted Hartree calculation in that all of the radial wave functions in a given shell are restricted to be identical and independent of spin projection. It is reasonable to expect that, as with lithium and a number of other cases, our calculated hfs coupling constant A will be in much closer agreement with experiment when the contributions of nuclear size and structure, and of the core electrons, are taken into account. The contribution of the core could be taken into account approximately, for example, through an unrestricted treatment in which the radial wave function may be spin-dependent.

The total potential due to the core $V_i(r)$ [Eq. (10)] in which the $6s$ electron moves will not differ greatly, however, between the restricted and the unrestricted treatments. Thus we stress the fact that the gold $6s_{1/2}$ wave function and the C_{nj} values which we have obtained here should be close to the correct values. On the other hand, the comparison of our calculated value for A with the measured value emphasizes the fact that, in estimating the charge density near the nucleus from a measured A, a substantial error will be made if the contributions to A of nuclear structure and of the core electrons are neglected.

We have also calculated $A_{6s}=A_{6s}(R_{\rm WS})$, the hfs coupling constant for the Wigner-Seitz atom. It was found, as expected, that $A_{6s}(R_{\rm WS})$ was proportional to $C_{6s}(R_{\rm WS})$ and displayed the same behavior as that shown for $C_{6s}(R_{\rm WS})$ in Fig. 1. In a complete calculation of $A(R_{\rm WS})$ it would, of course, be necessary to include the effects of core polarization, as discussed above. Here $A(R_{\rm WS})$ and $C(R_{\rm WS})$ would not in general have the same behavior with $R_{\rm WS}$.

E. Internal Conversion Coefficients for ^{169}Tm

The internal conversion coefficient α_{ns} in an ns shell is approximately proportional to C_{ns}. Thus $\alpha_{ns}/\alpha_{n's}\simeq C_{ns}/C_{n's}$. We have checked this relationship[35] for our calculated C_{ns} with measured relative intensities of the internal conversion electrons coming from the 8.4-keV transition of ^{169}Tm. The α and C ratios for the s-shell electrons were in agreement to within a few percent except where the valence shell was involved. We did not expect agreement in this latter case because chemical effects were not taken into account in the calculation of the C_{ns}. This agreement provides a kind of figure of merit for our calculated C_{ns} values, but a further comparison of our C_{ns} values with absolute experimental values for this quantity is, of course, desirable.

---

[28] H. Kopfermann, *Nuclear Moments* (Academic Press Inc., New York, 1958).
[29] E. Fermi and E. Segrè, Z. Physik **82**, 729 (1933).
[30] G. Wessel and H. Lew, Phys. Rev. **92**, 641 (1953).
[31] L. M. Sachs, Phys. Rev. **117**, 1504 (1960).
[32] R. K. Nesbet, Phys. Rev. **118**, 681 (1960).
[33] P. Kusch and H. Taub, Phys. Rev. **75**, 1477 (1949).
[34] R. K. Nesbet, Colloq. Intern. Centre Natl. Rech. Sci. (Paris) **164**, 87 (1967).
[35] T. A. Carlson, P. Erman, and K. Fransson, Nucl. Phys. **A111**, 371 (1968).

APPENDIX: NUMERICAL TREATMENT

We have endeavored to minimize errors resulting from the numerical treatment. We discuss here several areas in which we have used unusual numerical methods to this end.

It has generally been considered adequate to use the asymptotic, exponential solution of the Dirac equation [Eq. (1)] for all radii larger than that for which the wave functions reached an arbitrarily small value. For inner subshells, this radius is well within the atom, even for the Wigner-Seitz boundary condition. However, the terms of Eq. (1) which involve r^{-1} are far from zero at that point. Therefore, we solve Eq. (1) to the same outer boundary for all subshells to assure that the major and minor wave functions are in the proper ratio when they do become significant.

A second innovation, applicable only to the free-atom boundary condition, is closely related to the first. Rather than use the asymptotic ratio of major to minor component, Γ_∞, as the boundary value at the finite radius to which numerical integration is used, we have developed a series solution for Γ. By combining the two equations in (1), the differential equation for Γ can be written as

$$\frac{d\Gamma}{dr}=\left(\frac{2-\epsilon}{\alpha}+\alpha[V_N(r)-V_i(r)]\right)+\frac{2k}{r}\Gamma-\left(\frac{\epsilon}{\alpha}-\alpha[V_N(r)-V_i(r)]\right)\Gamma^2. \quad \text{(A1)}$$

If r is sufficiently large, the term $V_N(r)-V_i(r)$ can be replaced by the effective potential Z_e/r, where

$$Z_e=Z-N+1, \quad \text{(A2)}$$

and an asymptotic series can be obtained for Γ by substituting the formal series

$$\Gamma(r)=\sum_{n=0}^{\infty}\beta_n r^{-n} \quad \text{(A3)}$$

into Eq. (A1). The lowest-order coefficient β_0 is identically Γ_∞, and is given by

$$\Gamma_\infty=\beta_0=-[(2-\epsilon)/\epsilon]^{1/2} \quad \text{(A4)}$$

and the higher β_n can be calculated recursively from

$$\beta_{n+1}=\frac{(2k+n)\alpha\beta_n}{2\epsilon\beta_0}+\frac{\alpha^2 Z_e}{2\epsilon\beta_0}(\delta_{n0}+\sum_{k=0}^{n}\beta_{n-k}\beta_k)-\frac{1}{2\beta_0}\sum_{k=1}^{n}\beta_{n+1-k}\beta_k, \quad \text{(A5)}$$

with the convention that the second sum is zero for $n=0$. As an illustration of the need for using the asymptotic series in place of the first term, the following results were obtained for the 1*s* shell of lithium, with $r=50$ Bohr units (certainly well beyond any non-$1/r$ behavior of the potential),

$$\epsilon=1.317\times10^{-4}, \quad Z_e=1:$$

$$\beta_0=\lim_{r\to\infty}\Gamma(r)=-123.2,$$

$$\Gamma(r)=-122.6 \text{ [taking four terms of (A3)]}.$$

While these values differ by only 0.5%, the values obtained from the differential equation for $d\Gamma/dr$ are

$$d\Gamma/dr=-2.7 \quad (\Gamma=\beta_0),$$

$$d\Gamma/dr=-0.009 \quad [\Gamma=\Gamma(r)].$$

Thus starting only with the ratio Γ_∞ [i.e., only β_0 in (A3)], one may be close to the actual value, yet the slope of Γ could be wrong by orders of magnitude. It is therefore advisable to use the expansion (A3).

Since there exist linear multistep methods for the numerical solution of a single differential equation such that the error introduced at one step will decrease while the solution increases through succeeding steps, it is generally assumed that a system of differential equations having only increasing solutions may be solved accurately by one of these methods. Unfortunately, as shown by the analyses of Milne and Reynolds,[36] Crane and Klopfenstein,[37] and others, this assumption is not valid. Depending upon the eigenvalues of the coefficient matrix of the differential equation and upon the integration step size, a method which is stable for a single equation may cause exponential growth of errors previously introduced into a system of two or more equations. (Errors are always introduced by starting values, discretization, or round-off.) The coefficient matrix of the differential equation [Eq. (1)] for the radial wave functions is such that, for $\epsilon>\alpha^2[V_N(r)-V_i(r)]$, errors will grow exponentially, whether integrating inward or outward, unless the step size is very small (of the order $10^{-4}/\epsilon$ Bohr radii). Therefore, to avoid the prohibitively small step size necessary for performing the inward integration by a multistep method, we have used Gragg's[38] method of extrapolating the step size to zero. Using only the number of extrapolations needed to achieve a specified consistency in two successive extrapolations, the step size is automatically adjusted to the largest practical value. The inward integration is terminated at the greatest radius such that $\epsilon\leq\alpha^2\times[V_N(r)-V_i(r)]$ is satisfied, thus insuring that the outward integration may be performed accurately by a fast linear multistep procedure.[39]

---

[36] W. E. Milne and R. R. Reynolds, J. Assoc. Comp. Mach. **7**, 46 (1960).
[37] R. L. Crane and R. W. Klopfenstein, J. Assoc. Comp. Mach. **12**, 227 (1965).
[38] W. B. Gragg, J. SIAM Numer. Analyses **2**, 384 (1965).
[39] W. E. Milne and R. R. Reynolds, J. Assoc. Comp. Mach. **9**, 64 (1962).